Revealing the competition between peeled ssDNA, melting bubbles, and S-DNA during DNA overstretching by single-molecule calorimetry

Xinghua Zhang[a,b], Hu Chen[b], Shimin Le[b], Ioulia Rouzina[c], Patrick S. Doyle[a,d,1], and Jie Yan[a,b,e,f,1]

[a]BioSystems and Micromechanics Interdisciplinary Research Group, Singapore-MIT Alliance for Research and Technology, National University of Singapore, Republic of Singapore 138602; [b]Mechanobiology Institute, National University of Singapore, Republic of Singapore 117411; [c]Department of Biochemistry, Molecular Biology and Biophysics, University of Minnesota, Minneapolis, MN 55455; [d]Department of Chemical Engineering, Massachusetts Institute of Technology, Cambridge, MA 02139; [e]Department of Physics, National University of Singapore, Republic of Singapore 117542; and [f]Centre for Bioimaging Sciences, National University of Singapore, Republic of Singapore 117546

Edited by Vincent Croquette, École Normale Supérieure, Paris, France, and accepted by the Editorial Board January 16, 2013 (received for review August 8, 2012)

Double-stranded DNA (dsDNA) unconstrained by torsion undergoes an overstretching transition at about 65 pN, elongating the DNA to about 1.7-fold. Three possible structural transitions have been debated for the nature of DNA overstretching: (*i*) "peeling" apart of dsDNA to produce a peeled ssDNA strand under tension while the other strand coils, (*ii*) "inside-strand separation" of dsDNA to two parallel ssDNA strands that share tension (melting bubbles), and (*iii*) "B-to-S" transition to a novel dsDNA, termed S-DNA. Here we overstretched an end-opened DNA (with one open end to allow peeling) and an end-closed (i.e., both ends of the linear DNA are covalently closed to prohibit peeling) and torsion-unconstrained DNA. We report that all three structural transitions exist depending on experimental conditions. For the end-opened DNA, the peeling transition and the B-to-S transition were observed; for the end-closed DNA, the inside-strand separation and the B-to-S transition were observed. The peeling transition and the inside-strand separation are hysteretic and have an entropy change of approximately 17 cal/(K·mol), whereas the B-to-S transition is nonhysteretic and has an entropy change of approximately −2 cal/(K·mol). The force-extension curves of peeled ssDNA, melting bubbles, and S-DNA were characterized by experiments. Our results provide experimental evidence for the formation of DNA melting bubbles driven by high tension and prove the existence of nonmelted S-DNA. Our findings afford a full understanding of three possible force-driven structural transitions of torsion-unconstrained DNA and the resulting three overstretched DNA structures.

DNA bubble | magnetic tweezers

Double-stranded DNA (dsDNA) is a dynamic molecule whose structure depends on conditions. In addition to B-DNA, dsDNA can exist in several other structures, such as A-DNA and Z-DNA under certain solution conditions (1, 2). Recent rapid progress in single-DNA manipulation allows application of tension and torque to dsDNA, leading to discoveries of new dsDNA structures such as L-DNA, produced by stretching undertwisted DNA (3), or P-DNA, produced by stretching an overtwisted DNA (4). The DNA overstretching transition was originally observed on DNA with open ends (end-opened DNA), which is torsion-unconstrained (5, 6). Since its discovery, three transitions have been debated to explain DNA overstretching (4–21) (Fig. 1): (*i*) "peeling" of one strand from the other to a peeled ssDNA strand under tension while the other ssDNA strand coils, (*ii*) "inside-strand separation" to two parallel ssDNA strands that share tension (melting bubbles), and (*iii*) "B-to-S" transition to a novel overstretched dsDNA, termed S-DNA. To fully understand the nature of DNA overstretching, these possible structural transitions should be carefully examined.

For end-opened DNA, two kinetically and thermodynamically distinct overstretching transitions have been reported (6–12), which can be selected by changing base-pair stability through temperature, salt concentration, and DNA sequence (8–10). One transition is the peeling transition to peeled ssDNA (8–10, 18). This transition is hysteretic, with entropy change (ΔS) of about 20 cal/(K·mol) (10), which is consistent with the value of ΔS measured in traditional DNA thermal melting experiments (22). The other transition, however, is nonhysteretic with a slight negative ΔS of about −3 cal/(K·mol) (10). Although this ΔS is consistent with the formation of a highly ordered S-DNA, it might also be explained by the formation of melting bubbles if the backbones of the two ssDNA strands strongly interact with each other (10). Although the possibility of force-driven inside-strand separation was hypothesized theoretically (14), it has never been directly tested by experiments.

To determine whether the B-to-S transition and the force-driven inside-strand separation of DNA exist, and what experimental conditions the selection among the possible force-driven transitions of torsion-unconstrained DNA depends on, we applied a transverse magnetic tweezers setup (23) (Fig. 2*A*) to overstretch two designed DNA constructs at different salt concentrations and temperatures, characterized the kinetics of the transitions, and measured the force-extension curves of the overstretched DNA structures.

Results

Three Distinct Transitions Revealed by Kinetics and Micromechanics. Here, we systematically investigated three possible overstretching transitions for an end-opened DNA construct (Fig. 2*B*), with one open end to allow peeling, and an end-closed, torsion-unconstrained DNA construct of the same sequence (Fig. 2C), in which both ends of the linear DNA are covalently closed to prohibit peeling (20). For the end-opened DNA, all three transitions are allowed topologically, whereas for the end-closed DNA, only the B-to-S transition and inside-strand separation are allowed topologically. The methods to control temperature, force, and salt concentration are described in *SI Text*, Magnetic Tweezers Measurements and also described in the SI appendix of our previous publication (10).

As a reference, we first stretched the end-opened DNA molecule at 24 °C (Fig. 3*A*). Short DNA of about 7,300 bp was used to minimize the potential existence of nicks inside the DNA. The DNA molecule was tethered between the edge of a functionalized glass slide and a paramagnetic bead, and the extension of DNA was determined as the distance from the bead to the edge

Author contributions: X.Z. and J.Y. designed research; X.Z. and S.L. performed research; X.Z., H.C., I.R., P.S.D., and J.Y. analyzed data; and X.Z. and J.Y. wrote the paper.

The authors declare no conflict of interest.

Freely available online through the PNAS open access option.

This article is a PNAS Direct Submission. V.C. is a guest editor invited by the Editorial Board.

[1]To whom correspondence may be addressed. E-mail: phyyj@nus.edu.sg or pdoyle@mit.edu.

This article contains supporting information online at www.pnas.org/lookup/suppl/doi:10.1073/pnas.1213740110/-/DCSupplemental.

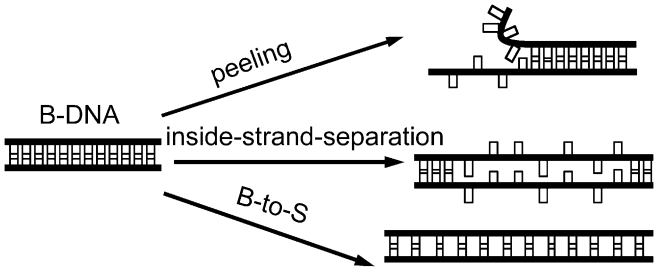

Fig. 1. Possible force-driven structural transitions of torsion-unconstrained DNA. Three possible structural transitions have been debated for the nature of DNA overstretching: peeling apart of dsDNA to produce an ssDNA strand under tension, inside-strand separation of dsDNA to two ssDNA strands that share tension, and B-to-S transition to a novel nonmelted S-DNA.

(Fig. 2*A*). The position of the bead was determined by its centroid (Fig. S1), and an offset based on the known force-extension curve of ssDNA (6, 11, 17) was used to find the absolute value of the DNA extension (Fig. 3*A* and *SI Text*, Additional Information for Fig. 3). We found that decreasing the NaCl concentration, which reduces base-pair stability, caused a switch from the nonhysteretic transition (overlapping force-extension curves obtained in force-increase and force-decrease scans) to the hysteretic peeling transition (nonoverlapping force-extension curves obtained in force-increase and force-decrease scans) (Fig. 3*A*). This result is consistent with the previous results obtained using end-opened 48,502-bp λ-DNA (6–10). Interestingly, the overstretched DNA is stiffer and shorter after the nonhysteretic transition at 150 mM NaCl (Fig. 3*A*, black) than after the hysteretic peeling transition at 1mM NaCl (Fig. 3*A*, blue). We also observed that at 20 mM NaCl (Fig. 3*A*, red) the extension of the overstretched DNA is in between those obtained at 150 mM NaCl and 1 mM NaCl, indicating the coexistence of two overstretched DNA structures at this intermediate salt concentration. Note that the extension offset does not affect the relative values of extension between the DNA structures after the nonhysteretic transition and after the peeling transition.

For the end-closed DNA, we found the nonhysteretic transition also occurred at ~60 pN in 150 mM and 20 mM NaCl (Fig. 3*B*) at 24 °C, which is consistent with the results Paik and Perkins (20) obtained using a similar end-closed DNA construct and Fu et al. (9) obtained on short DNA capped with two GC-rich ends to prohibit peeling. Decreasing the NaCl concentration to reduce base-pair stability of DNA caused a switch from the nonhysteretic transition to a hysteretic transition. When the concentration of NaCl was decreased to 1 mM, the extension of the DNA after the hysteretic transition approached that predicted for two parallel noninteracting ssDNA strands (Fig. 3*B*, indicated as 2ssDNA), in agreement with formation of melting bubbles where the two ssDNA strands share tension (17). The hysteretic transition is likely to be the inside-strand separation because the end-closed DNA does not allow peeling topologically. Notably, the hysteretic transition produced an overstretched DNA whose length was shorter than the DNA after the nonhysteretic transition for end-closed DNA. This length is also different from that found for the hysteretic peeling transition for end-opened DNA, which produced peeled ssDNA longer than the DNA after the nonhysteretic transition (Fig. 3*A*). At the intermediate NaCl concentration of 5 mM (Fig. 3*A*, olive), the force-extension curves of the overstretched DNA is in between those obtained at 150 mM NaCl and 1 mM NaCl, indicating the coexisting of two overstretched DNA structures.

In addition to decreasing salt concentration, lower base-pair stability can also be achieved by increasing temperature. We found that increasing temperature at 3.5 mM NaCl caused a switch from the nonhysteretic transition to a hysteretic transition of end-closed DNA (Fig. 3*C*). Because peeled ssDNA is not produced on end-closed DNA (Fig. 3 *B* and *C*), the offset to obtain the absolute values of DNA extension was based on the measured force-extension curve of the DNA after the nonhysteretic transition in 150 mM NaCl (Fig. 3*A* and *SI Text*, Additional Information for Fig. 3). Again, the extension offset does not affect the relative extensions between the DNA structures after the nonhysteretic transition or after the hysteretic transition.

Together with the switch from the nonhysteretic to the hysteretic transition of the end-closed DNA, the overstretched DNA switched from a more rigid structure to a less rigid structure (Fig. 3*D*). The stiffness of the overstretched DNA was calculated as the reciprocal of the slope in the force-extension curve at >70 pN (Fig. S2*A*), as a function of temperature at three NaCl concentrations. The data at 3.5 mM (Fig. 3*D*, olive squares) and 20 mM (Fig. 3*D*, red squares) NaCl were obtained from the same DNA molecule as that used in Fig. 3*C*. The data at 10 mM NaCl (Fig. 3*D*, blue triangles) were obtained from an independent end-closed DNA molecule to demonstrate the reproducibility of the switch of stiffness. At 3.5 mM NaCl, the stiffness of the overstretched DNA monotonically decreased with temperature from ~3 N/(m/bp) at ~12 °C, where the nonhysteretic transition dominated, to ~1 N/(m/bp) in the range of 28–37 °C, where the hysteretic transition dominated. At 20 mM NaCl, the stiffness of the overstretched DNA remained ~3 N/(m/bp) from ~12 °C to ~20 °C, where the nonhysteretic transition dominated. As the temperature was increased further, the stiffness of the overstretched DNA monotonically decreased to ~1 N/(m/bp) at ~35 °C, where the hysteretic transition dominated. At 10 mM NaCl, a decrease in the stiffness with increased temperature of the overstretched DNA was also observed. The two different values of stiffness of overstretched DNA suggest that different DNA structures were produced from the nonhysteretic transition and the hysteretic transition. The intermediate values of stiffness between ~3 N/(m/bp) and ~1 N/(m/bp) indicate the coexistence of two different overstretched DNA structures.

Taken together, our data demonstrate three distinct overstretched DNA structures by their different force-extension curves. For the end-opened DNA, the structure from the hysteretic transition has a force-extension curve consistent with an ssDNA strand, whereas on the end-closed DNA, the structure from the hysteretic transition has a force-extension curve consistent with two parallel, noninteracting ssDNA strands. In addition, for both the end-opened and end-closed DNA, a stiffer overstretched DNA structure was observed from the nonhysteretic transition, with an extension shorter than one ssDNA strand but longer than two parallel noninteracting ssDNA strands, which can be attributed to the formation of nonmelted S-DNA.

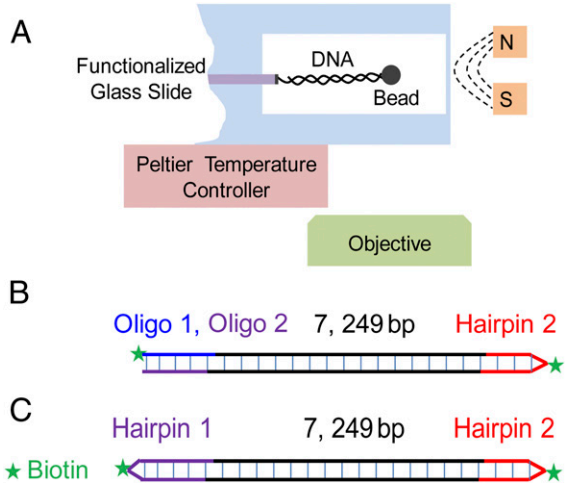

Fig. 2. Experimental setup. (*A*) Schematic of the transverse magnetic tweezers with temperature control. (*B*) End-opened DNA that allows peeling from the open end. (*C*) End-closed and torsion-unconstrained DNA (the same sequence as the end-opened DNA) that does not allow peeling topologically.

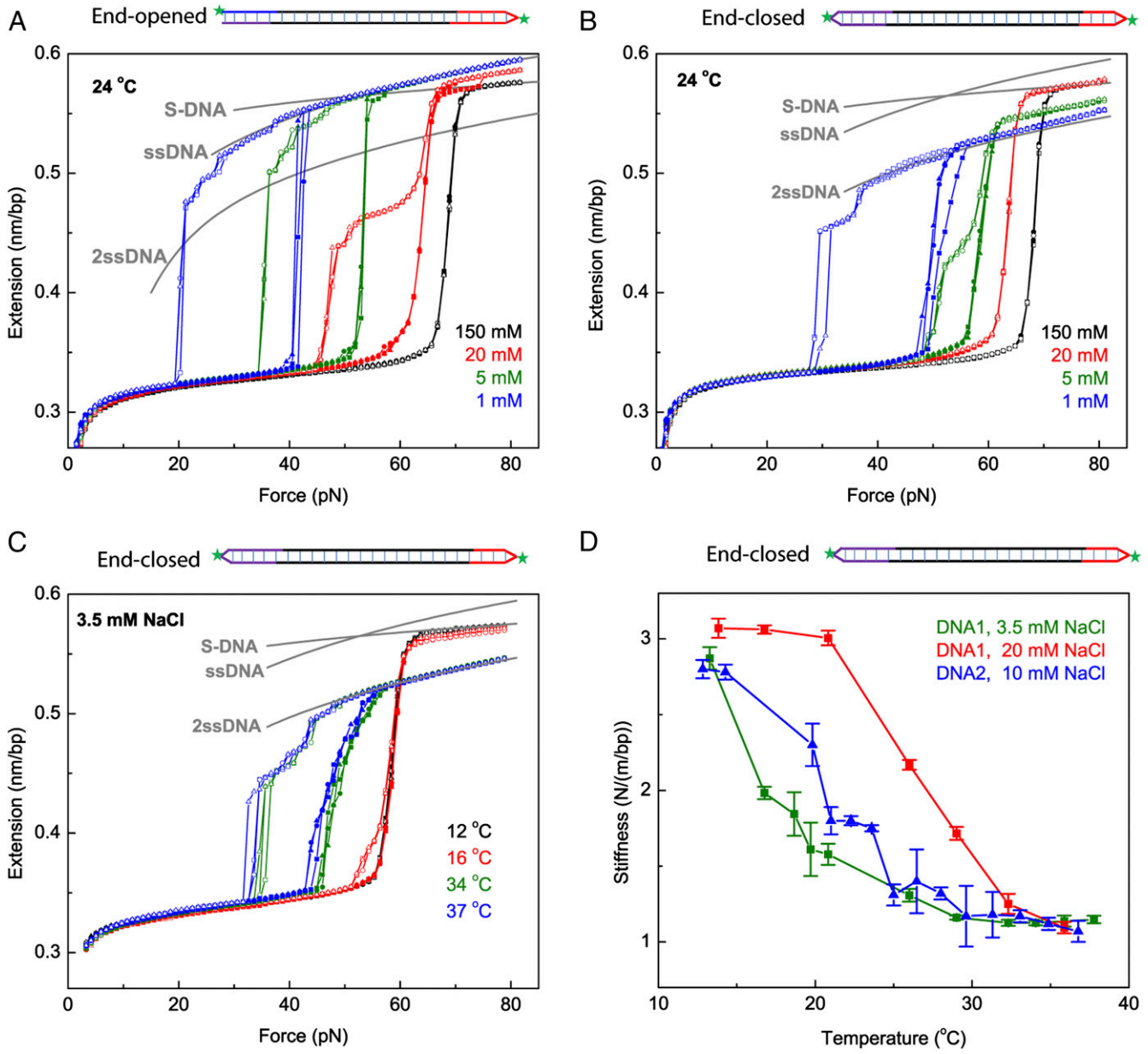

Fig. 3. Three distinct transitions revealed by force-extension curves of the end-opened and end-closed DNA. At each NaCl concentration and each temperature on each DNA molecule, a force-increase scan (~1 pN to ~80 pN, filled symbols) until transition finished was performed, followed by a force-decrease scan (~80 pN to ~1 pN, open symbols) through the same set of forces. The two scans generated two force-extension curves. The force scans were repeated three times, generating six force-extension curves. For each data record, the DNA was held for 1 s at a constant force, during which the extension was measured, and a loading rate of ±1 pN/s was used. (*A*) Force-extension curves of an end-opened DNA molecule at the indicated NaCl concentrations at a constant temperature of 24 °C. The force-extension curve of ssDNA produced in 1 mM NaCl is matched with the theoretical force-extension curve of ssDNA to determine the extension offset. The theoretical force-extension curve of two parallel noninteracting ssDNA strands (2ssDNA) is plotted for comparison. The force-extension curve of the S-DNA obtained at 150 mM was fitted to an extensible worm-like-chain (WLC) model with a persistence length of 13 nm, a stretching modulus of 2,700 pN, and contour length of 0.576 nm/bp. (*B*) Force-extension curves of an end-closed DNA molecule at the indicated NaCl concentrations at a constant temperature of 24 °C. The fitted WLC model of S-DNA in *A* was used to match the experimental S-DNA force-extension curve in 150 mM NaCl to determine the extension offset. The theoretical force-extension curves of ssDNA and 2ssDNA are plotted for comparison. (*C*) Force-extension curves of an end-closed DNA molecule at the indicated temperatures in 3.5 mM NaCl. The fitted WLC model of S-DNA was used to match the experimental S-DNA force-extension curve at 12 °C to determine the extension offset. The theoretical force-extension curves of ssDNA and 2ssDNA are plotted for comparison. (*D*) Stiffness of overstretched DNA as a function of temperature and NaCl concentration of end-closed DNA. At each NaCl concentration and each temperature on each DNA molecule, six force-extension curves were obtained as shown in *C*. The stiffness of the overstretched DNA was calculated for each of the six force-extension curves at forces greater than 70 pN. The average and SD of the six stiffness values were calculated and plotted as data points and error bars. The data at 3.5 mM (olive squares) and 20 mM (red squares) NaCl were obtain on the same DNA molecule as that was used for *C*. The data at 10 mM NaCl (blue triangles) were obtained on another end-closed DNA molecule to demonstrate the reproducibility.

Temperature Dependence of the Transition Force. To provide further insights into the nature of the nonhysteretic and hysteretic transitions of end-closed DNA, we applied single-molecule calorimetry measurements to determine ΔS and the enthalpy change (ΔH). Such measurements have the advantages of probing the intrinsic thermodynamic properties of the transitions, without potential

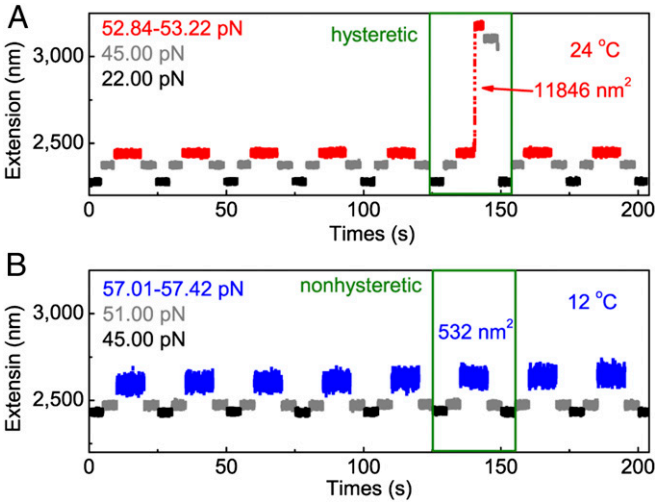

Fig. 4. Force-cycling procedure to determine the onset of the transition and transition types. All of the data shown were obtained using the same end-closed DNA molecule in 5 mM NaCl. The olive rectangle in each panel shows one force cycle during which the transition occurred, indicated by the variance in extension fluctuation greater than the preset threshold value of 500 nm^2 at the higher force. (*A*) Representative force-cycling procedure between 45 pN (gray) and higher forces of 52.84–53.22 pN (red) that increased by increments of ~0.05 pN at 24 °C. A lower force of 22 pN (black) was used to speed up the reannealing process. The extension of DNA did not return to the extension before transition immediately after the force was decreased to 45 pN, indicating hysteresis (olive rectangle). (*B*) A representative force-cycling between 51 pN (gray) and higher forces of 57.01–57.42 pN (blue) that increased by increments of ~0.06 pN at 12 °C. Hysteresis was not observed when the force returned to 51 pN (olive rectangle).

external perturbations to DNA structures. ΔS and ΔH during DNA overstretching can be directly determined by measurements of $F_t(T)$ using the following equations: $\Delta S = -(\partial F_t/\partial T)\Delta b$ and $\Delta G = \Delta\Phi + \Delta H - T\Delta S = 0$. Here, F_t is the transition force, T is the temperature, Δb is the DNA extension change per base pair during the transition, and $\Delta\Phi$ is the force-dependent free energy change that can be calculated with force-extension curves of B-DNA and the particular overstretched DNA structure (13) (*SI Text*, Calculation of Entropy and Enthalpy Changes).

To measure ΔS of a particular transition type, concurrence of different types of overstretching transitions should be avoided. Therefore, we chose to measure F_t at the onset of the overstretching transition where mostly only one type of transition can occur (10). The onset of a transition was probed by a force-cycling procedure, in which the force was cycled between a fixed force (45 pN in Fig. 4*A* and 51 pN in Fig. 4*B*) slightly below the transition and a series of increasing higher forces (52.84–53.22 pN in Fig. 4*A* and 57.01–57.42 pN in Fig. 4*B*). At each of the higher forces, the DNA was held at a constant force for a time window of 10 s, during which the extension of DNA and variance in extension fluctuation were measured. Analogous to other phase transitions, a clear signature at the onset of the overstretching transition is a dramatic increase in extension fluctuations. A threshold (500 nm^2) of the variance in extension fluctuation was used to mark the occurrence of the transitions (10).

In our setup, during each force-cycling procedure, the transition occurred stochastically and occurred more frequently at higher forces than at lower forces (Fig. S3), indicating that the transition was not at equilibrium in the finite time window of 10 s. At a finite time window, the smaller the force detected, the closer it is to the equilibrium transition force. Thus, the lowest transition force, which corresponded to the first time the transition was observed during the force-cycling procedure, was recorded (*SI Text*, Determination of the Onset of Transition and Transition Types). The procedure was repeated five times, yielding five lowest transition-force values. The average and the SD of the five lowest transition-force values were calculated and were plotted in Fig. 5 as a data point and error bar of F_t.

In addition to determining F_t, the transition type was simultaneously determined based on whether hysteresis was observed. As an example, in the force cycle [45 pN to 53.11 pN (transition occurred) to 45 pN] (Fig. 4*A*, olive rectangle), the extension of DNA did not return to the original B-DNA extension at 45 pN immediately after the force was decreased from 53.11 pN back to 45 pN, indicating hysteresis. Hence, the transition was determined to be a hysteretic transition. For comparison, hysteresis was not observed in the force cycle for 51 pN to 57.31 pN (transition occurred) to 51 pN (Fig. 4*B*, olive rectangle). Hence, the transition was determined to be a nonhysteretic transition. Data obtained in the nonhysteretic and hysteretic transitions were used to calculate ΔS separately. As the onset of any type of overstretching transition that occurs somewhere in the DNA molecule can be detected, this procedure probed one of the competing overstretching transitions that occurred at the lowest force. More than one type of transition may occur at elevated forces during DNA overstretching (olive and red, respectively, in Fig. 3 *B* and *C*).

Due to the slow kinetics and the stochastic nature of DNA melting (9, 19), the slope of $\partial F_t/\partial T$ measured may depend on the choice of the time window. The effect of the time window on

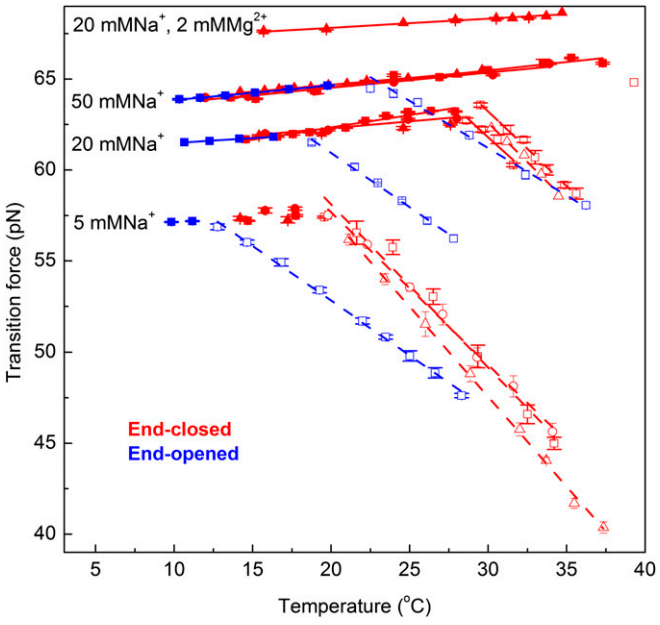

Fig. 5. Thermodynamics of the three distinct transitions revealed by measurements of $F_t(T)$ on the end-opened DNA and end-closed DNA. At each NaCl concentration and each temperature on each DNA molecule, five repeating force-cycling procedures were performed, yielding five lowest transition forces. The average and the SD of the five lowest transition-force values were calculated and plotted as a data point and error bar of F_t. In each salt concentration, two independent end-opened DNA molecules (indicated by squares and circles) and three independent end-closed DNA molecules (indicated by squares, circles, and triangles) were stretched to demonstrate the reproducibility. In the nonhysteretic B-to-S transition, F_t is denoted by filled symbols and fitted to a linear function (solid line) at each NaCl concentration on each DNA molecule to obtain the slope of $\partial F_t/\partial T$. Then, $\partial F_t/\partial T$ from different DNA molecules at each NaCl concentration were used to obtain the average and the SD of $\partial F_t/\partial T$ for the calculation of ΔS. In the hysteretic transition, F_t is denoted by open symbols and also fitted to a linear function (dashed line) at each NaCl concentration on each DNA molecule to obtain $\partial F_t/\partial T$. The slopes from independent DNA molecules at each NaCl concentration were used to obtain the average and the SD of $\partial F_t/\partial T$ for the calculation of ΔS.

$\partial F_t/\partial T$ in a scale of 1–10 s was examined and was found to be negligible (Fig. S4).

Thermodynamics of the Three Distinct Transitions. The values of ΔS during the hysteretic and nonhysteretic overstretching transitions of the end-opened λ-DNA have been extensively investigated in our previous publication (10). Here, we remeasured the values of ΔS for the end-opened short DNA molecules as a reference (Fig. 5, blue). In 20 mM NaCl, a piecewise linear $F_t(T)$ was revealed. The two slopes from the two independent DNA molecules yielded the average and SD of the slope of $\partial F_t/\partial T = 0.10 \pm 0.06$ pN/K at low temperatures where the nonhysteretic transition was observed, and $\partial F_t/\partial T = -0.56 \pm 0.06$ pN/K at high temperatures where the hysteretic peeling transition was observed. From $\partial F_t/\partial T$, Δb, the value of ΔS was determined to be -2.8 ± 1.7 cal/(K·mol) for the nonhysteretic transition and 16.0 ± 1.8 cal/(K·mol) for the hysteretic peeling transition of end-opened DNA (*SI Text*, Calculation of Entropy and Enthalpy Changes). These results are consistent with the data measured on the end-opened λ-DNA in our previous publication (10).

Similar piecewise linear $F_t(T)$ was also revealed for the end-closed DNA. In 20 mM NaCl, the results obtained from three independent DNA molecules yielded $\partial F_t/\partial T = 0.08 \pm 0.01$ pN/K at low temperatures where the nonhysteretic transition was observed, and $\partial F_t/\partial T = -0.83 \pm 0.04$ pN/K at high temperatures where the hysteretic transition was observed. The value of ΔS was determined to be -2.3 ± 0.2 cal/(K·mol) for the nonhysteretic transition and 16.6 ± 0.8 cal/(K·mol) for the hysteretic transition. Because magnesium exists in a millimolar concentration range in vivo, we also studied the effects of magnesium on overstretching of end-closed DNA. We found that the existence of 2 mM $MgCl_2$ in 20 mM NaCl could inhibit the hysteretic transition up to 35 °C and increase F_t by about 6 pN. Results obtained in other salt concentrations from both the end-opened and the end-closed DNA are summarized in Table 1. Details of the calculations for the values can be found in Fig. S5 and Tables S1–S4.

Discussion

In this study, three distinct force-driven structural transitions of torsion-unconstrained DNA were observed to depend on experimental conditions. For end-opened DNA, a nonhysteretic transition associated with a small negative ΔS and a hysteretic transition associated with a large positive ΔS were observed, which produced a shorter and a longer overstretched DNA, respectively. The switch from the nonhysteretic transition to the hysteretic transition occurred when increasing the temperature or when decreasing the salt concentration to decrease base-pair stability. Based on previous reports, the hysteretic transition of end-opened DNA was determined to be the peeling transition to peeled ssDNA (8–10, 18). The remaining question is whether the nonhysteretic transition is the inside-strand separation or the B-to-S transition.

This question was addressed by experiments on end-closed DNA. For end-closed DNA, our study demonstrated a nonhysteretic transition at high DNA base-pair stability (low temperature or high salt) associated with a small negative ΔS, and a hysteretic transition at lower DNA base-pair stability associated with a large positive ΔS. Because the peeling transition is not allowed on the end-closed DNA topologically, the two distinct transitions are either the inside-strand separation or the B-to-S transition. We conclude that the hysteretic transition is the inside-strand separation based on two observations: (*i*) The ΔS during the hysteretic transition agrees with the ΔS during DNA thermal melting, and (*ii*) the force-extension curve of the overstretching DNA after the hysteretic transition agrees with the theoretical prediction for two parallel, noninteracting ssDNA strands. This conclusion implies that the nonhysteretic transition is neither the peeling transition nor the inside-strand separation; in other words, the nonhysteretic transition is the B-to-S transition to base-paired S-DNA. The existence of S-DNA was also reported recently by Bosaeus et al. (24) on ultrashort DNA of only ∼60 bp, which occurs preferentially at GC-rich sequences and its relative extension is substantially shorter than that of peeled ssDNA.

In the same salt concentration, the values of ΔS obtained in the peeling transition and in the inside-strand separation are slightly smaller than the value of ΔS obtained in the traditional DNA thermal melting experiments (22) (Table 1), which can be attributed to a finite heat capacity increase during DNA melting (10, 13, 15). The small negative value of ΔS obtained in the nonhysteretic transition suggests that the resulting DNA has a highly ordered structure. In addition, the ΔH of ∼1 kcal/mol obtained in the nonhysteretic transition, which is about one order of magnitude smaller than that measured in the DNA melting transitions, suggests that much less bond breaking occurs than in DNA melting. We also found that the existence of magnesium could significantly favor the nonhysteretic transition of end-closed DNA (Fig. 5), which is similar to our previous results that the existence of magnesium could favor the nonhysteretic transition on end-opened λ-DNA (10), likely due to the enhancement of the DNA base-pair stability by magnesium (25).

The properties of the three overstretching transitions and the resulting three overstretched DNA structures are summarized as follows: (*i*) kinetically, the B-to-S transition is much faster than both the peeling transition and the inside-strand separation; (*ii*) thermodynamically, both the peeling transition and the inside-strand separation have large positive entropy change similar to DNA thermal melting, whereas the B-to-S transition is distinct from DNA melting, indicated by its unique small negative entropy change; and (*iii*) mechanically, DNA melting bubbles formed from the inside-strand separation has a force-extension curve consistent with the prediction for two parallel, noninteracting ssDNA strands, whereas the stiffer S-DNA is shorter than ssDNA but longer than DNA melting bubbles at 60–80 pN. These findings provide a full understanding of force-driven structural transitions of torsion-unconstrained DNA.

Our findings raise interesting questions regarding the structure and physiological functions of S-DNA. If S-DNA is a double-stranded, highly ordered structure, the issue of how the two strands are organized needs to be discussed. Previously, Leger et al. (4) found that torsion-constrained DNA does not undergo the overstretching transition at ∼65 pN, unless the DNA is underwound. From Leger's experiment, S-DNA is predicted to be a right-handed, double-helical structure with a helical pitch of ∼22 nm, which has been confirmed by Bryant et al. (16), and more recently

Table 1. Comparison of ΔS and ΔH between our results and those reported in thermal melting experiments

	End-opened DNA				End-closed DNA				Thermal melting 50% GC
	Nonhysteretic B-to-S		Hysteretic peeling		Nonhysteretic B-to-S		Hysteretic inside-strand separation		
Enthalpy and entropy changes	50 mM NaCl	20 mM NaCl	50 mM NaCl	20 mM NaCl	50 mM NaCl	20 mM NaCl	20 mM NaCl	5 mM NaCl	5–50
ΔS [cal/(K·mol)]	−2.4 ± 0.2	−2.8 ± 1.7	16.4 ± 2.0	16.0 ± 1.8	−2.3 ± 0.2	−2.4 ± 1.2	16.6 ± 0.8	18.3 ± 1.5	∼24
ΔH (kcal/mol)	1.1 ± 0.1	0.9 ± 0.5	6.3 ± 0.7	6.0 ± 0.7	1.1 ± 0.1	1.0 ± 0.4	5.8 ± 0.4	6.1 ± 0.8	8.2

by a high-resolution atomic force microscopy analysis of DNA that was overstretched using the molecular combing method (21). Although the physiological functions of S-DNA are not clear, we speculate that S-DNA may be a potential binding substrate for DNA binding ligands or proteins, such as YOYO-1, RecA, and Rad51 (26–28), that elongate the DNA backbone to a similar level as S-DNA.

In an effort to provide a full understanding about the force-driven structural transitions of torsion-unconstrained DNA, we worked together with King et al. (29) to use our complementary technologies to the fullest. We focused on the following two aspects: (*i*) micromechanics of the DNA structures after the respective transitions and (*ii*) thermodynamics and kinetics of the respective transitions. In our study, three distinct overstretched DNA structures were identified based on their different force-extension curves and rigidities. From the thermodynamic and the kinetic measurements, the natures of the three DNA structures were revealed. In parallel to our study, King et al. (29) visualized the three overstretched DNA structures with the aid of structural-specific DNA binding dyes, using fluorescence imaging methods combined with single-molecule manipulation. Using this method, the regions of the respective overstretched DNA structures in overstretched DNA molecules were localized with high sensitivity. The two studies both revealed three distinct overstretched DNA structures and together provide a full picture of the micromechanics of three overstretched DNA structures, their localizations on overstretched DNA, and also the thermodynamics and kinetics of the respective transitions.

Due to different experiment designs in the two studies, there are two main different observations between our data and that of King et al. (29). One difference is that different types of transitions may be observed at the same salt concentrations in the two studies. This difference can be explained by different DNA sequences and different temperatures in the two studies, both of which may change the base-pair stabilities and affect the selection of transition types (*SI Text*, Comparison with Parallel Fluorescence Study). The other difference is that when melting bubbles were visualized by fluorescence-labeled RPA binding (RPA is an ssDNA binding protein), King et al. did not observe significant hysteresis, and the overstretched DNA had an extension similar to that of S-DNA, whereas in our study hysteresis was observed during the inside-strand separation and the resulting overstretched DNA was significantly shorter than S-DNA. This difference might arise if the overstretched DNA in their study contains a mixture of S-DNA and a fraction of small DNA bubbles that could be detected by their highly sensitive fluorescence imaging method (*SI Text*, Comparison with Parallel Fluorescence Study). Despite these differences, we emphasize that the two studies make the same main conclusions about the existence of three distinct overstretched DNA structures and their localizations; together, the two studies provide a clear answer to the long-running debate over the nature of DNA overstretching.

Materials and Methods

Refer to *SI Text* for details. These include the magnetic tweezers measurements, the preparation of DNA constructs, the additional information for Fig. 3, the determination of the onset of transition and transition types, the calculation of entropy and enthalpy changes, and the comparison with the parallel fluorescence study. See also the SI appendix in our previous publication (10).

ACKNOWLEDGMENTS. We thank John Marko (Northwestern University), Graeme King (VU University Amsterdam), Erwin Peterman (VU University Amsterdam), and Gijs Wuite (VU University Amsterdam) for stimulating discussions. This research was supported by the National Research Foundation Singapore through the Singapore-MIT Alliance for Research and Technology's BioSystems and Micromechanics research programme and through the Mechanobiology Institute at the National University of Singapore.

1. Franklin RE, Gosling RG (1953) Molecular configuration in sodium thymonucleate. *Nature* 171(4356):740–741.
2. Wang AHJ, et al. (1979) Molecular structure of a left-handed double helical DNA fragment at atomic resolution. *Nature* 282(5740):680–686.
3. Sheinin M, Forth S, Marko JF, Wang MD (2011) Underwound DNA under tension: Structure, elasticity and sequence-dependent behaviors. *Phys Rev Lett* 107(10): 108102–108106.
4. Leger JF, et al. (1999) Structural transitions of a twisted and stretched DNA molecule. *Phys Rev Lett* 83(5):1066–1069.
5. Cluzel P, et al. (1996) DNA: An extensible molecule. *Science* 271(5250):792–794.
6. Smith SB, Cui Y, Bustamante C (1996) Overstretching B-DNA: The elastic response of individual double-stranded and single-stranded DNA molecules. *Science* 271(5250): 795–799.
7. Mao H, Arias-Gonzalez JR, Smith SB, Tinoco I, Jr., Bustamante C (2005) Temperature control methods in a laser tweezers system. *Biophys J* 89(2):1308–1316.
8. Fu H, Chen H, Marko JF, Yan J (2010) Two distinct overstretched DNA states. *Nucleic Acids Res* 38(16):5594–5600.
9. Fu H, et al. (2011) Transition dynamics and selection of the distinct S-DNA and strand unpeeling modes of double helix overstretching. *Nucleic Acids Res* 39(8):3473–3481.
10. Zhang X, Chen H, Fu H, Doyle PS, Yan J (2012) Two distinct overstretched DNA structures revealed by single-molecule thermodynamics measurements. *Proc Natl Acad Sci USA* 109(21):8103–8108.
11. Rief M, Clausen-Schaumann H, Gaub HE (1999) Sequence-dependent mechanics of single DNA molecules. *Nat Struct Biol* 6(4):346–349.
12. Calderon CP, Chen W-H, Lin K-J, Harris NC, Kiang CH (2009) Quantifying DNA melting transitions using single-molecule force spectroscopy. *J Phys Condens Matter* 21(3): 34114.
13. Rouzina I, Bloomfield VA (2001) Force-induced melting of the DNA double helix. 2. Effect of solution conditions. *Biophys J* 80(2):894–900.
14. Rouzina I, Bloomfield VA (2001) Force-induced melting of the DNA double helix 1. Thermodynamic analysis. *Biophys J* 80(2):882–893.
15. Williams MC, Wenner JR, Rouzina I, Bloomfield VA (2001) Entropy and heat capacity of DNA melting from temperature dependence of single molecule stretching. *Biophys J* 80(4):1932–1939.
16. Bryant Z, et al. (2003) Structural transitions and elasticity from torque measurements on DNA. *Nature* 424(6946):338–341.
17. Cocco S, Yan J, Léger JF, Chatenay D, Marko JF (2004) Overstretching and force-driven strand separation of double-helix DNA. *Phys Rev E Stat Nonlin Soft Matter Phys* 70(1 Pt 1):011910.
18. van Mameren J, et al. (2009) Unraveling the structure of DNA during overstretching by using multicolor, single-molecule fluorescence imaging. *Proc Natl Acad Sci USA* 106(43):18231–18236.
19. Gross P, et al. (2011) Quantifying how DNA stretches, melts and changes twist under tension. *Nat Phys* 7:731–736.
20. Paik DH, Perkins TT (2011) Overstretching DNA at 65 pN does not require peeling from free ends or nicks. *J Am Chem Soc* 133(10):3219–3221.
21. Maaloum M, Beker A-F, Muller P (2011) Secondary structure of double-stranded DNA under stretching: elucidation of the stretched form. *Phys Rev E Stat Nonlin Soft Matter Phys* 83(3 Pt 1):031903.
22. SantaLucia J, Jr. (1998) A unified view of polymer, dumbbell, and oligonucleotide DNA nearest-neighbor thermodynamics. *Proc Natl Acad Sci USA* 95(4):1460–1465.
23. Yan J, Skoko D, Marko JF (2004) Near-field-magnetic-tweezer manipulation of single DNA molecules. *Phys Rev E Stat Nonlin Soft Matter Phys* 70(1 Pt 1):011905.
24. Bosaeus N, et al. (2012) Tension induces a base-paired overstretched DNA conformation. *Proc Natl Acad Sci USA* 109(38):15179–15184.
25. McFail-Isom L, Shui XQ, Williams LD (1998) Divalent cations stabilize unstacked conformations of DNA and RNA by interacting with base pi systems. *Biochemistry* 37(49): 17105–17111.
26. Günther K, Mertig M, Seidel R (2010) Mechanical and structural properties of YOYO-1 complexed DNA. *Nucleic Acids Res* 38(19):6526–6532.
27. Chen ZC, Yang HJ, Pavletich NP (2008) Mechanism of homologous recombination from the RecA-ssDNA/dsDNA structures. *Nature* 453(7194):489–4.
28. Reymer A, Frykholm K, Morimatsu K, Takahashi M, Nordén B (2009) Structure of human Rad51 protein filament from molecular modeling and site-specific linear dichroism spectroscopy. *Proc Natl Acad Sci USA* 106(32):13248–13253.
29. King GA, et al. (2012) Revealing the competition between peeled ssDNA, melting bubbles, and S-DNA during DNA overstretching using fluorescence microscopy. *Proc Natl Acad Sci USA*, 10.1073/pnas.1213676110.